HHS Public Access

Author manuscript

Hepatology. Author manuscript; available in PMC 2017 January 01.

Published in final edited form as:

Hepatology. 2016 January ; 63(1): 173–184. doi:10.1002/hep.28251.

Activation of the p62-Keap1-NRF2 Pathway Protects against Ferroptosis in Hepatocellular Carcinoma Cells

Xiaofang Sun[1], **Zhanhui Ou**[1], **Ruochan Chen**[2], **Xiaohua Niu**[1], **De Chen**[1], **Rui Kang**[2], and **Daolin Tang**[1,2,*]

[1]Center for DAMP Biology, The Third Affiliated Hospital of Guangzhou Medical University, Guangzhou, Guangdong, 510510, China

[2]Department of Surgery, University of Pittsburgh Cancer Institute, University of Pittsburgh, Pittsburgh, Pennsylvania 15213, USA

Abstract

Ferroptosis is a recently-recognized form of regulated cell death caused by an iron-dependent accumulation of lipid reactive oxygen species. However, the molecular mechanisms regulating ferroptosis remain obscure. Here, we report that nuclear factor erythroid 2-related factor (NRF2) plays a central role in protecting hepatocellular carcinoma (HCC) cells against ferroptosis. Upon exposure to ferroptosis-inducing compounds (e.g., erastin, sorafenib, and buthionine sulfoximine), p62 expression prevented NRF2 degradation and enhanced subsequent NRF2 nuclear accumulation through inactivation of Kelch-like ECH-associated protein 1. Additionally, nuclear NRF2 interacted with the transcriptional coactivator small v-maf avian musculoaponeurotic fibrosarcoma oncogene homolog (Maf) proteins such as MafG and then activated transcription of quinone oxidoreductase 1 (NQO1), heme oxygenase-1 (HO1), and ferritin heavy chain 1 (FTH1). Knockdown of p62, NQO1, HO1, and FTH1 by RNAi in HCC cells promoted ferroptosis in response to erastin and sorafenib. Furthermore, genetic or pharmacologic inhibition of NRF2 expression/activity in HCC cells increased the anticancer activity of erastin and sorafenib *in vitro* and in tumor xenograft models.

Conclusion—These findings demonstrate novel molecular mechanisms and signaling pathways of ferroptosis. The status of NRF2 is a key factor that determines the therapeutic response to ferroptosis-targeted therapies in HCC cells.

Keywords

degradation; erastin; sorafenib; chemosensitivity; chemoresistance

Introduction

Hepatocellular carcinoma (HCC) in men is the second leading cause of cancer-related death worldwide (1). Treatment options for advanced HCC, including surgical resection and non-surgical therapies, are of limited effectiveness. Sorafenib, a multiple kinase inhibitor, is the first systemic therapy to improve survival in HCC and is now a standard treatment pending

Correspondence to: Daolin Tang (tangd2@upmc.edu).

approval by the U.S. Food and Drug Administration (FDA) for patients with unresectable HCC (2, 3). However, sorafenib has been shown to provide limited survival benefits, suggesting the existence of primary and acquired drug resistance mechanisms (4). Impaired types of regulated cell death (RCD) such as apoptosis have been shown to participate in the development of sorafenib resistance in HCC. Further understanding of the molecular mechanism of RCD has become an important step in developing new therapeutics for overcoming sorafenib resistance in HCC cells.

The nuclear factor erythroid 2-related factor 2 (NRF2) is a key regulator of the antioxidant response (5). Under unstressed conditions, low levels of NRF2 are primarily maintained by Kelch-like ECH-associated protein 1 (Keap1)-mediated proteasomal degradation. Under oxidative stress conditions, NRF2 protein is stabilized and initiates a multistep pathway of activation that includes nuclear translocation, heterodimerization with its partner small v-maf avian musculoaponeurotic fibrosarcoma oncogene homolog (Maf) proteins such as MafG, recruitment of transcriptional coactivators, and subsequent binding to antioxidant response elements of target genes (6). It is clear that NRF2 plays a dual role in the prevention or treatment of cancer, depending on the type and stage of the cancer (7, 8). For example, NRF2 prevents the initiation but accelerates the progression of chemical carcinogen- or oncogene-mediated carcinogenesis (9, 10). NRF2 overexpression inhibits apoptosis and contributes to chemoresistance in several cancers (11, 12). However, it is still unclear whether NRF2 activation is involved in the regulation of other forms of RCD, such as ferroptosis.

Ferroptosis, a form of RCD identified by Brent R. Stockwell's lab in 2012, is mediated by an iron-dependent accumulation of lipid reactive oxygen species (ROS) (13). Morphologic, biochemical, and genetic studies further highlight the unique aspects of ferroptosis in relation to apoptosis and other major forms of RCD (e.g., necroptosis and autophagic cell death) (13). For example, a caspase- and necrosome-independent pathway is required for ferroptosis to occur (13). In addition to mediated tissue injury and neuron death (14–16), induction of ferroptosis by preclinical (e.g., erastin) and clinical (e.g., sorafenib) drugs facilitates the selective elimination of several tumor cells and represents an emerging anticancer strategy (17–25). Several regulators of ferroptosis have recently been identified in certain cancer cells. For example, glutathione peroxidase 4 is a unique member of the selenium-dependent glutathione peroxidases in mammals with a pivotal role in inhibition of lipid ROS production during ferroptotic cancer death (20). Heat shock protein beta-1, a member of the molecular chaperones, can regulate actin filament dynamics and reduce cellular iron uptake in the induction of ferroptosis (24). More recently, p53 was found to act as a positive regulator of ferroptosis by inhibiting expression of SLC7A11 (a specific light chain subunit of the cystine/glutamate antiporter) (23). However, the critical signal transduction pathways and transcription regulators of ferroptosis remain elusive.

In this study, we demonstrated that the p62-Keap1-NRF2 pathway plays a central role in the protection of HCC cells against ferroptosis through upregulation of multiple genes (quinone oxidoreductase 1 [NQO1], heme oxygenase-1 [HO1], and ferritin heavy chain 1 [FTH1]) involved in iron and ROS metabolism. These target genes of NRF2 were negative regulators of ferroptosis because the knockdown of NQO1, HO1, and FTH1 increased growth

inhibition in HCC cells following ferroptotic inducers. Moreover, inhibition of NRF2 expression and activity *in vitro* and *in vivo* increased the anticancer activity of erastin and sorafenib in HCC cells. Collectively, our results indicate that NRF2 is a critical and novel transcription regulator of ferroptosis in HCC cells.

Materials and Methods

Antibodies and reagents

The antibodies to NRF2 (#12721), p-ERK1/2 (#4370), ERK (#9102), actin (#3700), glyceraldehyde 3-phosphate dehydrogenase (GAPDH, #5174), and β-tubulin (#2146) were obtained from Cell Signaling Technology (Danvers, MA, USA). The antibodies to NRF2 (#ab62352), Keap1 (#ab150654), and Lamin B1 (#ab16048) were obtained from Abcam (Cambridge, MA, USA). The antibodies to p62 (#sc-28359) and MafG (#sc-133770) were obtained from Santa Cruz. Cycloheximide (#C7698), MG-132 (#M7749), deferoxamine (#D9533), Z-VAD-FMK (#V116), necrostatin-1 (#N9037), and alkaloid trigonelline (#T5509) were obtained from Sigma (St. Louis, MO, USA). Necrosulfonamide (#480073) was obtained from EMD Millipore Corporation (Darmstadt, Germany). Erastin (#E7781), sorafenib (#S7397), ferrostatin-1 (#S7243), and liproxstatin-1 (#S7699) were obtained from Selleck Chemicals (Houston, TX, USA).

Cell culture

HepG2 (#HB-8065), Hepa1–6 (#CRL-1830), Hep3B (#HB-8064), and SNU-182 (#CRL-2235) cells were obtained from American Type Culture Collection. These cells were grown in Eagle's Minimum Essential Medium (HepG2 and Hep3B) or Dulbecco's Modified Eagle's Medium (Hepa1–6) or RPMI-1640 Medium (SNU-182) with 10% fetal bovine serum, 2 mM L-glutamine, and 100 U/ml of penicillin and streptomycin.

Cell viability analysis

Cell viability was evaluated with an alamarBlue Cell Viability Assay Kit (#88952, Thermo Fisher Scientific Inc. Rockford, IL, USA) according the manufacturer's instructions. In brief, cells were plated in a 96-well plate and exposed to various concentrations of the cytotoxic compounds for indicated times. The alamarBlue Reagent (10 μl) was added to each well and incubated at 37°C in 5% CO_2 for four hours, and then the plates were measured at 545 nm/590 nm (Ex/Em) using the Tecan Safire^2 Multi-detection Microplate Reader (Morrisville NC, USA). Average percentage of inhibition at each concentration was calculated as previously described.

Western blot analysis

Western blot was used to analyze protein expression as described previously (26). In brief, after extraction, proteins in cell lysates were first resolved by SDS-polyacrylamide gel electrophoresis and then transferred to nitrocellulose membrane and subsequently incubated with the primary antibody. After incubation with peroxidase-conjugated secondary antibodies, the signals were visualized by enhanced chemiluminescence (Pierce, Rockford, IL, USA, #32106) according to the manufacturer's instructions. Validation of the correct

NRF2 band using MG132 or another proteasome inhibitor of NRF2 as a control would be optimal.

RNAi and gene transfection

The human NRF2-shRNA (also termed NRF2-shRNA1 in Figure S1, SHCLNG-NM_006164_ TRCN0000007558; Sequence: CCGGCCGGCATTTCACTAAACACAACTCGAGTTGTGTTTAGTGAAATGCCGGTTTTT); human-shRNA2 (SHCLNG-NM_006164_TRCN0000007555; Sequence: CCGGGCTCCTACTGTGATGTGAAATCTCGAGATTTCACATCACAGTAGGAGCTTTTT); mouse NRF2-shRNA (SHCLNG-NM_010902_ TRCN0000054658; Sequence: CCGGCCAAAGCTAGTATAGCAATAACTCGAGTTATTGCTATACTAGCTTTGGTTTTTG); human Keap1-shRNA (SHCLNG-NM_012289_ TRCN0000156676; Sequence: CCGGGTGGCGAATGATCACAGCAATCTCGAGATTGCTGTGATCATTCGCCACTTTTTTG); mouse Keap1-shRNA (SHCLNG-NM_016679_TRCN0000295014; Sequence: CCGGCCTGCAACTCGGTGATCAATTCTCGAGAATTGATCACCGAGTTGCAGGTTTTTG); human p62-shRNA (SHCLNG-NM_003900_ TRCN0000007237; Sequence: CCGGCCTCTGGGCATTGAAGTTGATCTCGAGATCAACTTCAATGCCCAGAGGTTTTT); mouse p62-shRNA (SHCLNG-NM_011018_TRCN0000098619; Sequence: CCGGGAGGTTGACATTGATGTGGAACTCGAGTTCCACATCAATGTCAACCTCTTTTTG); human NQO1-shRNA (SHCLNG-NM_000903_ TRCN0000350362; Sequence: CCGGCGAGTCTGTTCTGGCTTATAACTCGAGTTATAAGCCAGAACAGACTCGTTTTTG); mouse NQO1-shRNA (SHCLNG-NM_008706_TRCN0000041864; Sequence: CCGGCCGAGTCATCTCTAGCATATACTCGAGTATATGCTAGAGATGACTCGGTTTTTG); human HO1-shRNA (SHCLNG-NM_002133_TRCN0000290436; Sequence: CCGGGCTGAGTTCATGAGGAACTTTCTCGAGAAAGTTCCTCATGAACTCAGCTTTTTG); mouse HO1-shRNA (SHCLNG-NM_010442_TRCN0000234076; Sequence: CCGGAGCCACACAGCACTATGTAAACTCGAGTTTACATAGTGCTGTGTGGCTTTTTTG); human FTH1-shRNA (SHCLNG-NM_002032_TRCN0000029432; Sequence: CCGGCCTGTCCATGTCTTACTACTTCTCGAGAAGTAGTAAGACATGGACAGGTTTTT); and mouse FTH1-shRNA (SHCLNG-NM_010239_TRCN0000340558; Sequence: CCGGGACTTCATTGAGACGTATTATCTCGAGATAATACGTCTCAATGAAGTCTTTTTG) were obtained from Sigma. Transfections were performed with Lipofectamine™ 3000 (#L3000008, Invitrogen) according the manufacturer's instructions.

Quantitative real time polymerase chain reaction

Total RNA isolation and quantitative RT-PCR (Q-PCR) were carried out using previously-described procedures (27). Briefly, first-strand cDNA synthesis was carried out by using a Reverse Transcription System Kit according to the manufacturer's instructions (#11801-025, OriGene Technologies, Rockville, MD, USA). cDNA from various cell samples was amplified with specific primers (human NRF2: 5′-CACATCCAGTCAGAAACCAGTGG-3′ and 5′-GGAATGTCTGCGCCAAAAGCTG-3′; mouse NRF2: 5′-CAGCATAGAGCAGGACATGGAG-3′ and 5′-GAACAGCGGTAGTATCAGCCAG-3′; human NQO1: 5′-CCTGCCATTCTGAAAGGCTGGT-3′ and 5′-GTGGTGATGGAAAGCACTGCCT-3′; mouse NQO1: 5′-GCCGAACACAAGAAGCTGGAAG-3′ and 5′-GGCAAATCCTGCTACGAGCACT-3′;

human HO1: 5′-CCAGGCAGAGAATGCTGAGTTC-3′ and 5′-AAGACTGGGCTCTCCTTGTTGC-3′; mouse HO1: 5′-CACTCTGGAGATGACACCTGAG-3′ and 5′-GTGTTCCTCTGTCAGCATCACC-3′; human FTH1: 5′-TGAAGCTGCAGAACCAACGAGG-3′ and 5′-GCACACTCCATTGCATTCAGCC-3′; mouse FTH1: 5′-GCCGAGAAACTGATGAAGCTGC-3′ and 5′-GCACACTCCATTGCATTCAGCC-3′; human FTL: 5′-TACGAGCGTCTCCTGAAGATGC-3′ and 5′-GGTTCAGCTTTTTCTCCAGGGC-3′; human DMT1: 5′-AGCTCCACCATGACAGGAACCT-3′ and 5′-TGGCAATAGAGCGAGTCAGAACC-3′; human TFR1: 5′-ATCGGTTGGTGCCACTGAATGG-3′ and 5′-ACAACAGTGGGCTGGCAGAAAC-3′; human FP1: 5′-GAGACAAGTCCTGAATCTGTGCC-3′ and 5′-TTCTTGCAGCAACTGTGTCACAG-3′) and the data was normalized to actin RNA (human: 5′-CACCATTGGCAATGAGCGGTTC-3′ and 5′-AGGTCTTTGCGGATGTCCACGT -3′; mouse: 5′-CATTGCTGACAGGATGCAGAAGG-3′ and 5′-TGCTGGAAGGTGGACAGTGAGG-3′).

Iron assay

The relative iron concentration in cell lysates was assessed using an Iron Assay Kit (#ab83366, Abcam) according to the manufacturer's instructions.

Lipid peroxidation assay

The relative malondialdehyde (MDA) concentration in cell lysates was assessed using a Lipid Peroxidation (MDA) Assay Kit (#ab118970, Abcam) according the manufacturer's instructions.

Glutathione assay

The relative glutathione (GSH) concentration in cell lysates was assessed using a Glutathione Assay Kit (#CS0260, Sigma) according the manufacturer's instructions.

NRF2 transcriptional activity assay

The transcriptional activity of NRF2 was assayed using the Cignal Antioxidant Response Reporter (luc) Kit (#CCS-5020L, Qiagen) according the manufacturer's instructions.

Animal models

All animal experiments were approved by the Institutional Animal Care and Use Committees and performed in accordance with the Association for Assessment and Accreditation of Laboratory Animal Care guidelines (http://www.aaalac.org).

To generate murine subcutaneous tumors, 1×10^6 Hepa1–6 cells in control shRNA or NRF2 knockdown cells in 200 μl phosphate buffered saline were injected subcutaneously to the right of the dorsal midline in C57BL/6 mice. Once the tumors reached 80–100 mm^3 at day seven, mice were randomly allocated into groups and treated with erastin (30 mg/kg intraperitoneal injection [i.p.], twice every other day) and sorafenib (10 mg/kg i.p., once every other day) for two weeks. On day 22 after start of treatment, tumors were removed.

Tumors were measured twice weekly and volumes were calculated using the formula length×width^2×π/6.

In another experiment, C57BL/6 mice were injected subcutaneously with indicated Hepa1–6 cells (1×10^6 cells/mouse) and treated with erastin (30 mg/kg i.p., twice every other day) and sorafenib (10 mg/kg i.p., once every other day) with or without the alkaloid trigonelline (1 mg/kg i.p., once every other day) at day seven for two weeks. On day 22 after the start of treatment, tumors were removed. Tumors were measured twice weekly and volumes were calculated using the formula length×width^2×π/6.

Statistical analysis

Unless otherwise indicated, data are expressed as means ± SD of three independent experiments. Unpaired Student's t tests were used to compare the means of two groups. One-way ANOVA was used for comparison among the different groups. When ANOVA was significant, *post hoc* testing of differences between groups was performed using the LSD test. A P-value < 0.05 was considered significant.

Results

Increased NRF2 expression levels during ferroptosis

Similar to results from previous studies (13, 17–20), erastin-, buthionine sulfoximine (BSO)-, and sorafenib-mediated cell death in human (HepG2) and mouse (Hepa1–6) HCC lines was blocked by ferrostatin-1 (a potent ferroptosis inhibitor), but not ZVAD-FMK (a potent apoptosis inhibitor) and necrosulfonamide (a potent necroptosis inhibitor) (Figure 1A). Lipid peroxidation is a key event in ferroptosis (28). As expected, the end products of lipid peroxidation, such as MDA, were significantly increased following treatment with erastin, BSO, and sorafenib (Figure 1B). Moreover, ferrostain-1, but not ZVAD-FMK and necrosulfonamide, inhibited MDA production in the induction of ferroptosis (Figure 1B). Oxidative stress, including lipid peroxidation, has been a major inducer of NRF2 expression. In order to examine whether the induction of ferroptosis by erastin, BSO, and sorafenib regulates NRF2 expression, we next analyzed protein and mRNA expression levels of NRF2 in HCC cells. Remarkably, treatment with these ferroptosis stimulants significantly induced NRF2 protein expression (Figure 1C), but not its mRNA expression (Figure 1D), indicating that induction of NRF2 expression in ferroptosis occurs in a transcription-independent manner. Furthermore, we used cycloheximide (a chemical protein synthesis inhibitor) or MG-132 (a selective 26S proteosomal inhibitor) to address the transcription-independent mechanism in NRF2 protein induction during ferroptosis. As a result, we found that cycloheximide limited whereas MG-132 augmented the increased NRF2 protein level by erastin in HepG2 cells (Figure 1E). To further determine the effects of erastin on NRF2 protein stability, the half-life of NRF2 protein was calculated in the erastin-treated and non-erastin-treated HepG2 cells. Indeed, erastin treatment prolonged the half-life of NRF2 (Figure 1F). Collectively, these findings suggest that NRF2 protein is stabilized in ferroptosis through the inhibition of NRF2 degradation.

Interaction between p62 and Keap1 regulates NRF2 expression levels during ferroptosis

Recently, studies have demonstrated that the substrate adaptor p62 (also called sequestosome 1) protein modulates NRF2 expression levels by directly interacting with Keap1 under stressors, including liver damage (29). Based on this, we next examined the effects of p62 on the regulation of NRF2 expression levels in ferroptosis. The p62 protein level did not significantly change, whereas the Keap1 protein level significantly decreased in response to erastin and sorafenib (Figure 2A). Moreover, the interaction between p62 and Keap1 increased following erastin and sorafenib treatment as shown by immunoprecipitation assay (Figure 2B). In contrast, we did not observe a significantly increased interaction between Keap1 and dipeptidyl peptidase 3 (another Keap1-interacting protein involved in the NRF2 pathway) following administration of erastin and sorafenib (data not shown). Next, we investigated whether p62 binds Keap1 to displace NRF2, thus inhibiting NRF2 degradation. Indeed, knockdown of p62 by shRNA promoted accumulation of Keap1 protein (Figure 2C), increased interaction between Keap1 and NRF2 (Figure 2D), and enhanced degradation of NRF2 (Figure 2C) in response to erastin and sorafenib. Moreover, knockdown of Keap1 by shRNA reversed loss of p62-increased degradation of NRF2 following erastin treatment (Figure 2E). Collectively, these findings suggest that the interaction between p62 and Keap1 is responsible for NRF2 expression levels in ferroptosis.

NRF2 expression contributes to ferroptosis resistance

To investigate whether upregulated NRF2 confers resistance to ferroptosis induced by erastin and sorafenib, we first measured cell viability when NRF2 is knocked down by specific shRNA (Figure 3A). Indeed, suppression of NRF2 expression by RNAi significantly promoted erastin- and sorafenib-induced growth inhibition in several human and mouse HCC cells (Figure 3B and **S1**) with increased ferroptotic events, including GSH depletion (Figure 3C), lipid ROS production (Figure 3C), and an increase of iron levels (Figure 3C). Several ferroptosis inhibitors (ferrostain-1 and liproxstatin-1) significantly reversed erastin- and sorafenib-induced growth inhibition in the absence of NRF2 (Figure 3D). ZVAD-FMK (a pan-caspase inhibitor), necrostatin-1 (a potent necroptosis inhibitor that targets receptor-interacting protein 1), and necrosulfonamide (a potent necroptosis inhibitor that targets mixed lineage kinase domain-like protein) did not significantly reverse this process (Figure 3D). In contrast, ZVAD-FMK inhibited staurosporine-induced apoptosis, whereas necrostatin-1 and necrosulfonamide inhibited tumor necrosis factor α-induced necroptosis in the presence of ZVAD-FMK (data not shown). These findings suggest that loss of NRF2 enhanced ferroptosis, but not apoptosis and necroptosis, following treatment with erastin and sorafenib. Similarly, knockdown of p62 by RNAi suppressed erastin- and sorafenib-induced NRF2 expression (Figure 2C) and promoted growth inhibition (Figure 3B) with increased ferroptotic events including GSH depletion (Figure 3C), lipid ROS production (Figure 3C), and an increase of iron levels (Figure 3C). In contrast, knockdown of Keap1 by RNAi reversed loss of p62-increased degradation of NRF2 in ferroptosis (Figure 2E). As expected, Keap1 knockdown led to resistance to erastin- and sorafenib-induced growth inhibition (Figure 3B) with decreased ferroptotic events (Figure 3C) in the absence or presence of p62 knockdown. Thus, the levels of NRF2 determine ferroptosis-mediated cell death. Moreover, sorafenib-induced downregulation of

phosphorylated ERK1/2 did not change after suppression of NRF2 expression in HepG2 cells (Figure S2), suggesting that the kinase-inhibitory activity of sorafenib is not regulated by NRF2 in HCC.

NRF2 activation contributes to ferroptosis resistance

To further characterize the role of NRF2 in ferroptosis, we investigated NRF2 activation during ferroptosis. Erastin and sorafenib induced the nuclear translocation of NRF2 (Figure 4A) and increased the activity of the NRF2 promoter-luciferase reporter (Figure 4B), suggesting that the activation of NRF2 is increased in response to ferroptosis stimuli. NRF2 heterodimerizes with small Maf nuclear proteins and binds to antioxidant response elements to activate a battery of cytoprotective genes against various injuries and toxic insults (30). The interaction between NRF2 and MafG was increased in response to erastin and sorafenib (Figure 4C). Given that ferroptosis is an iron- and ROS-dependent form of non-apoptotic cell death, we focused on analyzing mRNA expression of the prototypical NRF2 target gene quinone oxidoreductase 1 (NQO1) and other target genes involved in heme and iron metabolism (e.g., HO1, divalent metal transporter 1 (DMT1), transferrin receptor 1 (TFR1), ferritin light chain (FTL), FTH1, and ferroportin 1(FP1)] by Q-PCR. Among them, the expression of NQO1, HO1, and FTH1 were significantly upregulated in response to erastin and sorafenib, whereas knockdown of NRF2 inhibited the expression of these genes (Figure 4D). Importantly, knockdown of NQO1, HO1, and FTH1 by specific shRNA increased erastin- and sorafenib-induced growth inhibition (Figure 4E). Moreover, the alkaloid trigonelline (a potent NRF2 inhibitor (31)) also blocked the expression of NQO1, HO1, and FTH1 and increased growth inhibition (Figure 4F) following treatment with erastin and sorafenib. Collectively, these findings suggest that NRF2 transcriptional activation contributes to ferroptosis resistance partly through increased gene expression involved in heme, iron, and ROS metabolism.

Suppression of NRF2 enhanced ferroptosis in vivo

To determine whether suppression of NRF2 enhances ferroptosis *in vivo*, NRF2 knockdown mouse Hepa1–6 cells were implanted into the subcutaneous space of the right flank of mice. Beginning at day seven, these mice were treated with erastin and sorafenib. Compared with the control shRNA group, erastin and sorafenib treatment effectively reduced the size of tumors formed by NRF2 knockdown cells (Figure 5A) with decreased mRNA expression of NQO1, HO1, and FTH1 (Figure 5B). Q-PCR analysis of the expression of prostaglandin-endoperoxide synthase 2 (PTGS2), a marker for the assessment of ferroptosis *in vivo* (20), indicated that the knockdown of NRF2 increases ferroptosis (Figure 5B). Similarly, the alkaloid trigonelline also enhanced the anticancer activity of erastin and sorafenib in subcutaneous xenograft models (Figure 5C), which was associated with increased PTGS2 and decreased NQO1, HO1, and FTH1 expression (Figure 5D). Collectively, these results indicated that genetic and pharmacological inhibition of NRF2 expression rendered HCC more sensitive to erastin and sorafenib, showing that NRF2 plays a critical role in ferroptosis resistance *in vivo*.

Discussion

Drug resistance (both primary and acquired) is one of the most important hallmarks of cancer; some new therapeutic strategies focus on developing novel targeted therapy. Ferroptosis is a form of cell death that has recently been reported during exposure to erastin and other FDA-approved drugs, including sorafenib (13). In this study, we provide novel evidence that the p62-Keap1-NRF2 antioxidative signaling pathway is a key negative regulator of ferroptosis in HCC cells by transcriptional activation of genes involved in ROS and iron metabolism. Inhibition of the p62-Keap1-NRF2 pathway significantly enhanced the anticancer activity of erastin and sorafenib in HCC cells *in vitro* and *in vivo*.

The mode of cell death depends on the sources, targets, and effects of oxidative damage (28). For example, it has been suggested that apoptosis, a well-studied process of programmed cell death, is mainly regulated by mitochondrial respiratory chain-dependent generation of mitochondrial ROS. In contrast, ferroptosis involves generation of iron-dependent accumulation of lipid ROS, which can be pharmacologically inhibited by iron chelators (e.g., deferoxamine and desferrioxamine mesylate) and lipid peroxidation inhibitors (e.g., ferrostatin and liproxstatin) (13, 14). Therefore, understanding of the mechanisms of ROS-induced ferroptosis and how this process relates to tumorigenesis and cancer therapy could lead to the development of successful therapies.

Our current study indicates that the p62-Keap1-NRF2 antioxidative signaling pathway is involved in the protection of ferroptosis in HCC cells. p62 expression prevents NRF2 degradation and enhances subsequent NRF2 nuclear accumulation through inactivation of Keap1. The p62 protein recognizes many proteins, which is then scavenged by a sequestration process known as autophagy. However, the interplay between autophagy and ferroptosis remains unknown. NRF2, an important antioxidative transcriptional factor, regulates the expression of a number of cytoprotective genes involved in detoxification and antioxidant and drug metabolism via binding with its response element, the antioxidant response element. We demonstrate that NRF2-mediated anti-ferroptosis activity depends on the induction of NQO1, HO1, and FTH1. NQO1 and HO1 are antioxidants that are upregulated in response to erastin and sorafenib. Suppression of NQO1 and HO1 expression significantly increased ferroptosis in HCC cells, indicating that the balance between ROS and antioxidant levels is critical in the development of ferroptosis. An early study showed that ferroptosis-sensitive cells have increased TFR1 and decreased ferritin (FTL and FTH1) expression compared to ferroptosis-resistant cells (32). Our current study indicates that FTH1, but not FTL and TFR1, is regulated by NRF2 in ferroptosis. Like knockdown of NRF2, knockdown of FTH1 enhanced ferroptosis sensitivity, indicating that reduced iron storage may contribute to iron overload during ferroptosis. Moreover, iron overload can generate ROS via Fenton reaction. In addition to mediating cell death by induction of oxidative stress, excessive iron in the liver may act in carcinogenesis by facilitating tumor growth and modifying the immune system (33). Thus, it is important to keep in mind that induction of ferroptosis in the liver may have a different role in tumorigenesis and cancer therapy.

SLC7A11 is a key component of system X_c^-, an amino acid antiporter that typically mediates the exchange of extracellular L-cystine and intracellular L-glutamate across the cellular plasma membrane. p53 (especially acetylation-defective mutant $p53^{3KR}$) is responsible for the inhibition of SLC711A expression in ferroptosis (23). Suppression of SLC7A11 leads to GSH depletion and increased ferroptosis following erastin treatment (23). Interestingly, other studies have indicated that SLC7A11 is a transcriptional target of NRF2 (34, 35). Thus, other genes such as SLC7A11 may be involved in the NRF2-mediated protection of ferroptosis, which needs further investigation.

Sorafenib, marketed as Nexavar by Bayer, is a drug approved for the treatment of advanced renal cell carcinoma (primary kidney cancer). It has also received “fast track” FDA review/approval designation for the treatment of advanced HCC. Of note, several kinase inhibitors (e.g., erlotinib, gefitinib, tivantinib, vemurafenib, selumetinib, rapamycin, imatinib, masatinib, and ponatinib) with targets similar to those of sorafenib cannot induce ferroptosis in cancer cells (17, 18). Structure activity relationship analysis of sorafenib analogs indicates that sorafenib induces ferroptosis via a non-kinase target. Our current study also indicates that NRF2 does not change the kinase-inhibitory activity of sorafenib. Like erastin, sorafenib inhibits system X_c^- function and results in GSH depletion (18). Our data clearly show that suppression of NRF2 expression increases sorafenib-induced GSH depletion in HCC cells.

Importantly, our study shows that pharmacological or genetic inhibition of NRF2 by the alkaloid trigonelline or NRF2 shRNA significantly enhances the anticancer activity of erastin and sorafenib in HCC cells and tumor xenograft models. Trigonelline is an alkaloid present in considerable amounts in coffee and fenugreek seed. Numerous pharmacological activities have been attributed to trigonelline, including hypoglycemia and hypolipidemia (36). Recently, trigonelline has been reported to act against NRF2 (37) and enhance the chemotherapy sensitivity of etoposide in pancreatic cancer (31). The data presented here demonstrate that the alkaloid trigonelline has the potency to be used in combination therapy for liver cancer by overcoming chemoresistance in the induction of ferroptosis. It will be important to determine whether blocking the NRF2 pathway enhances ferroptotic cancer cell death in other mouse models of liver cancer such as genetically-engineered mouse models.

In summary, the present study provided the first evidence that activation of NRF2 inhibits ferroptosis in HCC cells (Figure 6). First, p62-mediated Keap1 degradation contributed to NRF2 activation in ferroptosis. Second, the NRF2-regulated genes NQO1, HO1, and FTH1 conferred ferroptosis resistance by modifying iron metabolism and lipid peroxidation. Finally, inhibition of NRF2 activation rendered HCC cells more susceptible to ferroptosis *in vitro* and *in vivo*. Functional characterization of the p62-Keap1-NRF2 pathway in ferroptosis may provide insight into the treatment of liver cancer.

Supplementary Material

Refer to Web version on PubMed Central for supplementary material.

Acknowledgments

Financial Support: This work was supported by the National Institutes of Health (R01CA160417 and R01GM115366 to D.T.), The National Natural Science Foundation of China (31171229 and U1132005 to X.S.), and a Science and Information Technology of Guangzhou Key Project (GZ2011Y1-00038\20140000000-4,3 to X.S.).

We thank Christine Heiner (Department of Surgery, University of Pittsburgh) for her critical reading of the manuscript.

List of Abbreviations

ROS	reactive oxygen species
NRF2	nuclear factor erythroid 2-related factor
Keap1	Kelch-like ECH-associated protein 1
Maf	v-maf avian musculoaponeurotic fibrosarcoma oncogene homolog
RCD	regulated cell death
NQO1	quinone oxidoreductase 1
HO1	heme oxygenase-1
FTH1	ferritin heavy chain 1
HCC	hepatocellular carcinoma
FDA	U.S. Food and Drug Administration
Q-PCR	quantitative real time polymerase chain reaction
BSO	buthionine sulfoximine
MDA	malondialdehyde
DMT1	divalent metal transporter 1
TFR1	transferrin receptor 1
FTL	ferritin light chain
FP1	ferroportin 1
GAPDH	glyceraldehyde 3-phosphate dehydrogenase
i.p	intraperitoneal injection

References

1. Jemal A, Bray F, Center MM, Ferlay J, Ward E, Forman D. Global cancer statistics. CA Cancer J Clin. 2011; 61:69–90. [PubMed: 21296855]
2. Llovet JM, Ricci S, Mazzaferro V, Hilgard P, Gane E, Blanc JF, de Oliveira AC, et al. Sorafenib in advanced hepatocellular carcinoma. N Engl J Med. 2008; 359:378–390. [PubMed: 18650514]
3. Abou-Alfa GK, Schwartz L, Ricci S, Amadori D, Santoro A, Figer A, De Greve J, et al. Phase II study of sorafenib in patients with advanced hepatocellular carcinoma. J Clin Oncol. 2006; 24:4293–4300. [PubMed: 16908937]
4. Zhai B, Sun XY. Mechanisms of resistance to sorafenib and the corresponding strategies in hepatocellular carcinoma. World J Hepatol. 2013; 5:345–352. [PubMed: 23898367]

5. Ma Q. Role of nrf2 in oxidative stress and toxicity. Annu Rev Pharmacol Toxicol. 2013; 53:401–426. [PubMed: 23294312]
6. Suzuki T, Motohashi H, Yamamoto M. Toward clinical application of the Keap1-Nrf2 pathway. Trends Pharmacol Sci. 2013; 34:340–346. [PubMed: 23664668]
7. Sporn MB, Liby KT. NRF2 and cancer: the good, the bad and the importance of context. Nat Rev Cancer. 2012; 12:564–571. [PubMed: 22810811]
8. Jaramillo MC, Zhang DD. The emerging role of the Nrf2-Keap1 signaling pathway in cancer. Genes Dev. 2013; 27:2179–2191. [PubMed: 24142871]
9. Satoh H, Moriguchi T, Takai J, Ebina M, Yamamoto M. Nrf2 prevents initiation but accelerates progression through the Kras signaling pathway during lung carcinogenesis. Cancer Res. 2013; 73:4158–4168. [PubMed: 23610445]
10. DeNicola GM, Karreth FA, Humpton TJ, Gopinathan A, Wei C, Frese K, Mangal D, et al. Oncogene-induced Nrf2 transcription promotes ROS detoxification and tumorigenesis. Nature. 2011; 475:106–109. [PubMed: 21734707]
11. Ren D, Villeneuve NF, Jiang T, Wu T, Lau A, Toppin HA, Zhang DD. Brusatol enhances the efficacy of chemotherapy by inhibiting the Nrf2-mediated defense mechanism. Proc Natl Acad Sci U S A. 2011; 108:1433–1438. [PubMed: 21205897]
12. Wang XJ, Sun Z, Villeneuve NF, Zhang S, Zhao F, Li Y, Chen W, et al. Nrf2 enhances resistance of cancer cells to chemotherapeutic drugs, the dark side of Nrf2. Carcinogenesis. 2008; 29:1235–1243. [PubMed: 18413364]
13. Dixon SJ, Lemberg KM, Lamprecht MR, Skouta R, Zaitsev EM, Gleason CE, Patel DN, et al. Ferroptosis: an iron-dependent form of nonapoptotic cell death. Cell. 2012; 149:1060–1072. [PubMed: 22632970]
14. Friedmann Angeli JP, Schneider M, Proneth B, Tyurina YY, Tyurin VA, Hammond VJ, Herbach N, et al. Inactivation of the ferroptosis regulator Gpx4 triggers acute renal failure in mice. Nat Cell Biol. 2014; 16:1180–1191. [PubMed: 25402683]
15. Linkermann A, Skouta R, Himmerkus N, Mulay SR, Dewitz C, De Zen F, Prokai A, et al. Synchronized renal tubular cell death involves ferroptosis. Proc Natl Acad Sci U S A. 2014; 111:16836–16841. [PubMed: 25385600]
16. Skouta R, Dixon SJ, Wang J, Dunn DE, Orman M, Shimada K, Rosenberg PA, et al. Ferrostatins inhibit oxidative lipid damage and cell death in diverse disease models. J Am Chem Soc. 2014; 136:4551–4556. [PubMed: 24592866]
17. Lachaier E, Louandre C, Godin C, Saidak Z, Baert M, Diouf M, Chauffert B, et al. Sorafenib induces ferroptosis in human cancer cell lines originating from different solid tumors. Anticancer Res. 2014; 34:6417–6422. [PubMed: 25368241]
18. Dixon SJ, Patel DN, Welsch M, Skouta R, Lee ED, Hayano M, Thomas AG, et al. Pharmacological inhibition of cystine-glutamate exchange induces endoplasmic reticulum stress and ferroptosis. Elife. 2014; 3:e02523. [PubMed: 24844246]
19. Louandre C, Ezzoukhry Z, Godin C, Barbare JC, Maziere JC, Chauffert B, Galmiche A. Iron-dependent cell death of hepatocellular carcinoma cells exposed to sorafenib. Int J Cancer. 2013; 133:1732–1742. [PubMed: 23505071]
20. Yang WS, SriRamaratnam R, Welsch ME, Shimada K, Skouta R, Viswanathan VS, Cheah JH, et al. Regulation of ferroptotic cancer cell death by GPX4. Cell. 2014; 156:317–331. [PubMed: 24439385]
21. Yagoda N, von Rechenberg M, Zaganjor E, Bauer AJ, Yang WS, Fridman DJ, Wolpaw AJ, et al. RAS-RAF-MEK-dependent oxidative cell death involving voltage-dependent anion channels. Nature. 2007; 447:864–868. [PubMed: 17568748]
22. Dolma S, Lessnick SL, Hahn WC, Stockwell BR. Identification of genotype-selective antitumor agents using synthetic lethal chemical screening in engineered human tumor cells. Cancer Cell. 2003; 3:285–296. [PubMed: 12676586]
23. Jiang L, Kon N, Li T, Wang SJ, Su T, Hibshoosh H, Baer R, et al. Ferroptosis as a p53-mediated activity during tumour suppression. Nature. 2015; 520:57–62. [PubMed: 25799988]
24. Sun X, Ou Z, Xie M, Kang R, Fan Y, Niu X, Wang H, et al. HSPB1 as a novel regulator of ferroptotic cancer cell death. Oncogene. 2015

25. Yu Y, Xie Y, Cao L, Yang L, Yang M, Lotze MT, Zeh HJ, et al. The Ferroptosis Inducer Erastin Enhances Sensitivity of Acute Myeloid Leukemia Cells to Chemotherapeutic Agents. Molecular & Cellular Oncology. 2015

26. Tang D, Kang R, Livesey KM, Kroemer G, Billiar TR, Van Houten B, Zeh HJ 3rd, et al. High-mobility group box 1 is essential for mitochondrial quality control. Cell Metab. 2011; 13:701–711. [PubMed: 21641551]

27. Yang L, Xie M, Yang M, Yu Y, Zhu S, Hou W, Kang R, et al. PKM2 regulates the Warburg effect and promotes HMGB1 release in sepsis. Nat Commun. 2014; 5:4436. [PubMed: 25019241]

28. Dixon SJ, Stockwell BR. The role of iron and reactive oxygen species in cell death. Nat Chem Biol. 2014; 10:9–17. [PubMed: 24346035]

29. Komatsu M, Kurokawa H, Waguri S, Taguchi K, Kobayashi A, Ichimura Y, Sou YS, et al. The selective autophagy substrate p62 activates the stress responsive transcription factor Nrf2 through inactivation of Keap1. Nat Cell Biol. 2010; 12:213–223. [PubMed: 20173742]

30. Itoh K, Chiba T, Takahashi S, Ishii T, Igarashi K, Katoh Y, Oyake T, et al. An Nrf2/small Maf heterodimer mediates the induction of phase II detoxifying enzyme genes through antioxidant response elements. Biochem Biophys Res Commun. 1997; 236:313–322. [PubMed: 9240432]

31. Arlt A, Sebens S, Krebs S, Geismann C, Grossmann M, Kruse ML, Schreiber S, et al. Inhibition of the Nrf2 transcription factor by the alkaloid trigonelline renders pancreatic cancer cells more susceptible to apoptosis through decreased proteasomal gene expression and proteasome activity. Oncogene. 2013; 32:4825–4835. [PubMed: 23108405]

32. Yang WS, Stockwell BR. Synthetic lethal screening identifies compounds activating iron-dependent, nonapoptotic cell death in oncogenic-RAS-harboring cancer cells. Chem Biol. 2008; 15:234–245. [PubMed: 18355723]

33. Kowdley KV. Iron, hemochromatosis, and hepatocellular carcinoma. Gastroenterology. 2004; 127:S79–86. [PubMed: 15508107]

34. Sasaki H, Sato H, Kuriyama-Matsumura K, Sato K, Maebara K, Wang H, Tamba M, et al. Electrophile response element-mediated induction of the cystine/glutamate exchange transporter gene expression. J Biol Chem. 2002; 277:44765–44771. [PubMed: 12235164]

35. Mitsuishi Y, Taguchi K, Kawatani Y, Shibata T, Nukiwa T, Aburatani H, Yamamoto M, et al. Nrf2 redirects glucose and glutamine into anabolic pathways in metabolic reprogramming. Cancer Cell. 2012; 22:66–79. [PubMed: 22789539]

36. Zhou J, Chan L, Zhou S. Trigonelline: a plant alkaloid with therapeutic potential for diabetes and central nervous system disease. Curr Med Chem. 2012; 19:3523–3531. [PubMed: 22680628]

37. Boettler U, Sommerfeld K, Volz N, Pahlke G, Teller N, Somoza V, Lang R, et al. Coffee constituents as modulators of Nrf2 nuclear translocation and ARE (EpRE)-dependent gene expression. J Nutr Biochem. 2011; 22:426–440. [PubMed: 20655719]

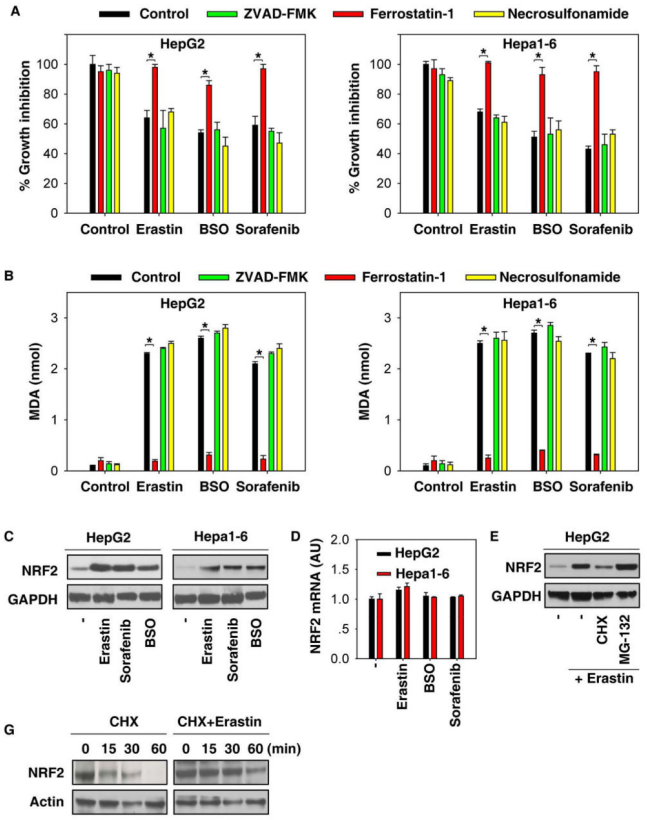

Figure 1. Increased NRF2 expression levels during ferroptosis

(A, B) Indicated HCC cells were treated with erastin (10 μM), BSO (200 μM), and sorafenib (5 μM) with or without indicated inhibitors (ZVAD-FMK,10 μM; ferrostatin-1, 1 μM; necrosulfonamide, 0.5 μM) for 24 hours and cell viability (A) and MDA levels (B) were assayed (n=3, *p < 0.05). (C, D) Indicated HCC cells were treated with erastin (10 μM), BSO (200 μM), and sorafenib (5 μM) for 24 hours and NRF2 protein (C) and mRNA (D) levels were assayed (n=3, *p < 0.05). (E) HepG2 cells were treated with erastin (10 μM) with or without cycloheximide (“CHX”, 20μg/ml) or MG-132 (5 μM) for 24 hours and NRF2 protein level was assayed. (F) HepG2 cells were treated with 20 μg/ml CHX over a 1h time period (left) or treated with 10 μM erastin for 4h followed by 20 μg/ml CHX over a 1h time period. Cells were lysed at the indicated time points. Cell lysates were subjected to western blot analysis with anti-NRF2 and anti-actin antibodies.

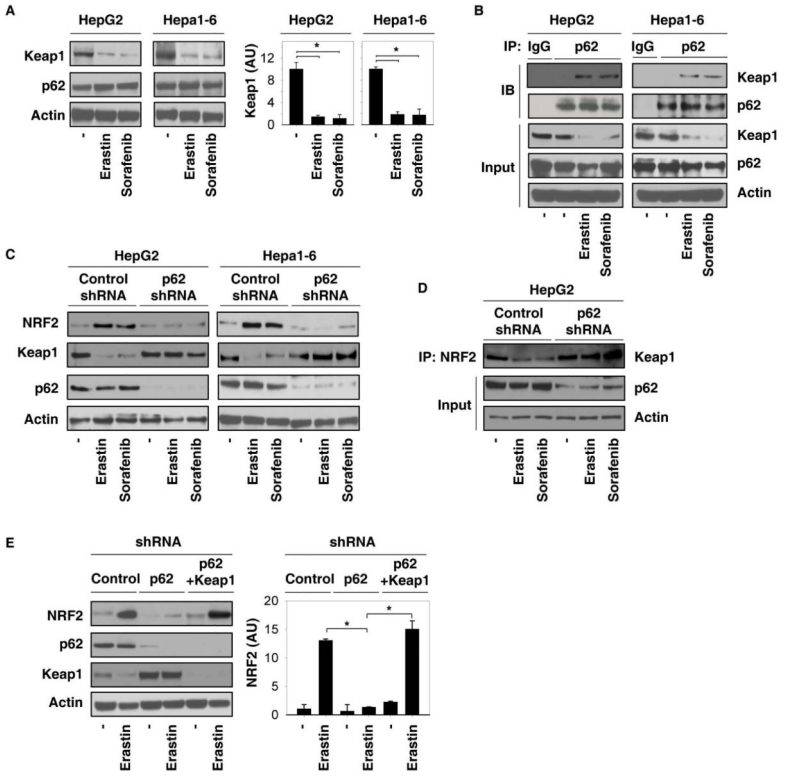

Figure 2. Interaction between p62 and Keap1 regulates NRF2 expression levels during ferroptosis

(A, B) Indicated HCC cells were treated with erastin (10 μM) and sorafenib (5 μM) for 24 hours. The protein levels of Keap1 and p62 (A), as well as interaction between Keap1 and p62 (B), were assayed using western blot and immunoprecipitation (IP) (n=3, *p < 0.05). (C, D) Indicated p62 knockdown HCC cells were treated with erastin (10 μM) and sorafenib (5 μM) for 24 hours. The protein levels of NRF2, Keap1, and p62 (C), as well as the interaction between NRF2 and Keap1 (D), were assayed with western blot and IP. (E) Knockdown of Keap1 by shRNA reversed loss of p62-inceased degradation of NRF2 following erastin (10 μM) treatment in HepG2 cells.

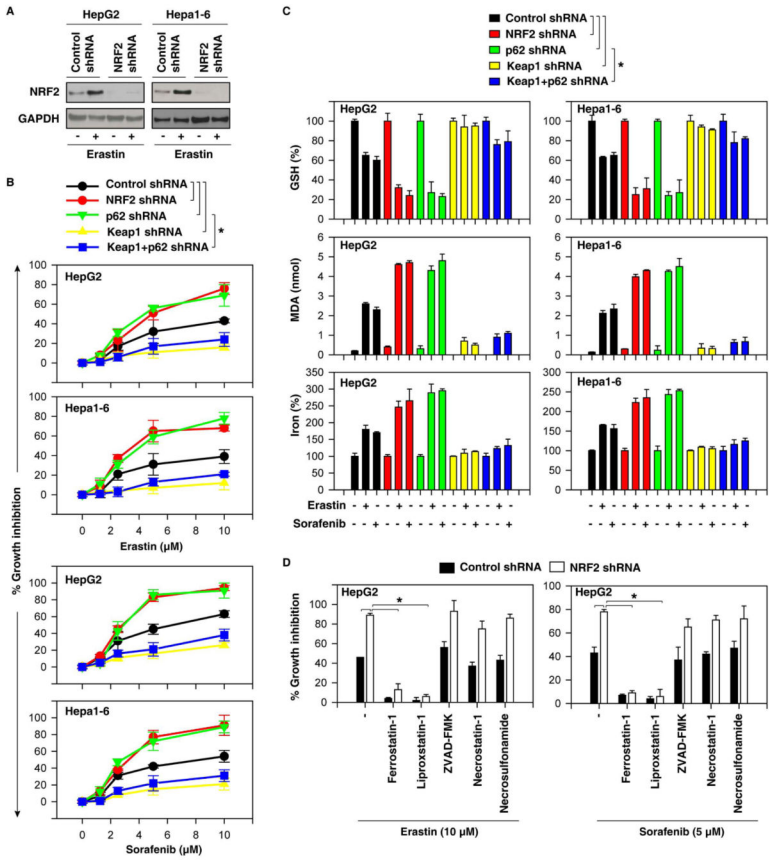

Figure 3. NRF2 expression contributes to ferroptosis resistance

(A) Western blot analysis of NRF2 expression in indicated NRF2 knockdown HCC cells. (B) Indicated knockdown HCC cells were treated with erastin (1.25–10 μM) and sorafenib (1.25–10 μM) for 24 hours and cell viabilities were assayed (n=3, *p < 0.05). (C) Indicated knockdown HCC cells were treated with erastin (10 μM) and sorafenib (5 μM) for 24 hours and GSH, MDA, and iron levels were assayed (n=3, *p < 0.05). (D) Indicated NRF2 knockdown HCC cells were treated with erastin (10 μM) and sorafenib (5 μM) with or without indicated inhibitors (ferrostatin-1, 1 μM; liproxstatin-1, 100nM; ZVAD-FMK,10 μM; necrostatin-1, 10 μM; necrosulfonamide, 0.5 μM) for 24 hours and cell viability was assayed (n=3, *p < 0.05).

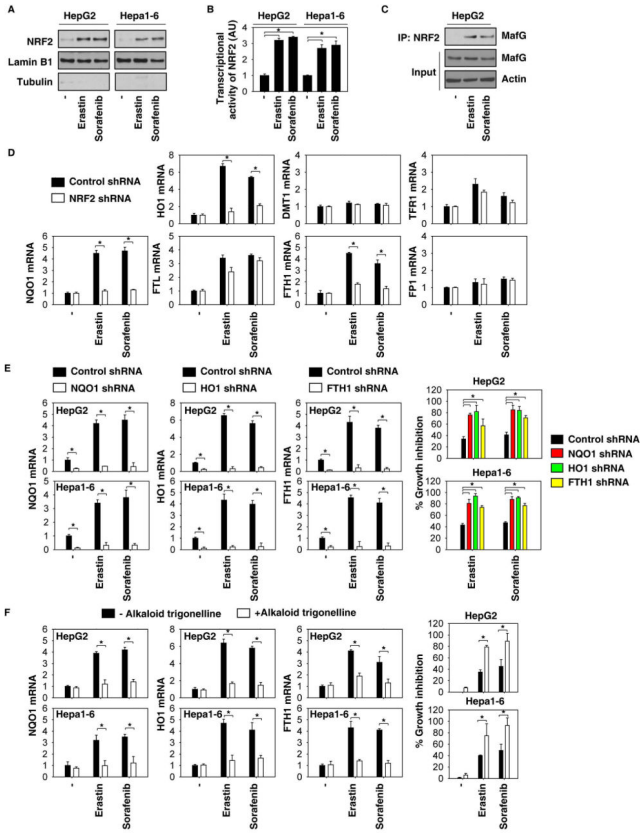

Figure 4. NRF2 activation contributes to ferroptosis resistance

(A–C) Indicated HCC cells were treated with erastin (10 μM) and sorafenib (5 μM) for 24 hours. The expression of NRF2 in nuclear extracts (A), transcription activity of NRF2 (B), and interaction between NRF2 and MafG (C) were assayed (n=3, *p < 0.05). (D) Indicated NRF2 knockdown HCC cells were treated with erastin (10 μM) and sorafenib (5 μM) for 24 hours. The mRNA expression of NQO1, HO1, and FTH1 were assayed by Q-PCR (n=3, *p < 0.05). (E) Knockdown of NQO1, HO1, and FTH1 by specific shRNA enhanced growth inhibition in indicated HCC cells following treatment with erastin (10 μM) and sorafenib (5 μM) for 24 hours (n=3, *p < 0.05). (F) The NRF2 inhibitor alkaloid trigonelline (0.5 μM) inhibited NQO1, HO1, and FTH1 mRNA expression and enhanced growth inhibition in indicated HCC cells following treatment with erastin (10 μM) and sorafenib (5 μM) for 24 hours (n=3, *p < 0.05).

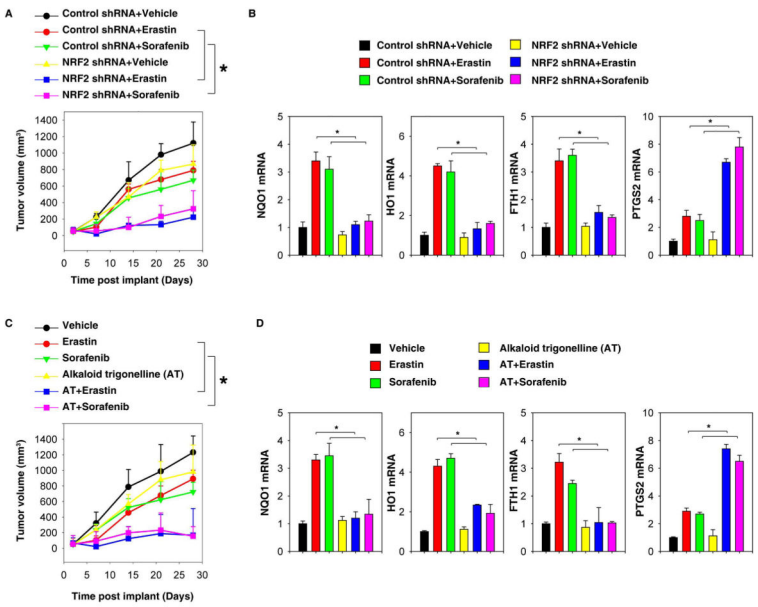

Figure 5. Suppression of NRF2 enhances ferroptosis *in vivo*

(A, B) NRF2 knockdown Hepa1–6 cells were more sensitive to erastin and sorafenib *in vivo*. (A) C57BL/6 mice were injected subcutaneously with indicated Hepa1–6 cells (1×10^6 cells/mouse) and treated with erastin (30 mg/kg i.p., twice every other day) and sorafenib (10 mg/kg i.p., once every other day) at day seven for two weeks. Tumor volume was calculated weekly. Data represents mean ± SE (n=5–8 mice/group, * $p < 0.05$). (B) Q-PCR analysis of the indicated gene expression in isolated tumor at day 28. (C, D) The alkaloid trigonelline increased the anticancer activity of erastin and sorafenib *in vivo*. (C) C57BL/6 mice were injected subcutaneously with indicated Hepa1–6 cells (1×10^6 cells/mouse) and treated with erastin (30 mg/kg i.p., twice every other day) and sorafenib (10 mg/kg i.p., once every other day) with or without the alkaloid trigonelline (1 mg/kg i.p., once every other day) at day seven for two weeks. Tumor volume was calculated weekly. Data represent mean ± SE (n=5–8 mice/group, * $p < 0.05$). (D) Q-PCR analysis of the indicated gene expression in isolated tumor at day 28.

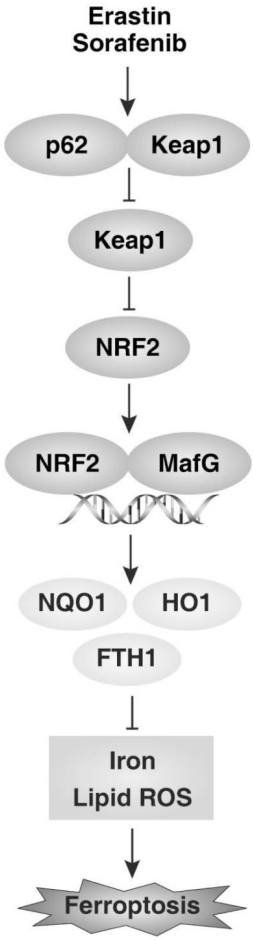

Figure 6.
Activation of NRF2 confers resistance to ferroptosis in hepatocellular carcinoma cells.